Tellus (1987), *39A*, 385–389

On the contrasting influence of organized moist convection and surface heat flux on a barotropic vortex

By HANS ØKLAND and HARALD SCHYBERG, *Institute of Geophysics, University of Oslo, P.O. Box 1022 Blindern, N-0315 Oslo 3, Norway*

(Manuscript received 23 June; in final form 27 November 1986)

ABSTRACT

The paper describes an experiment in which a barotropic vortex is heated either by convection connected to the convergence of water vapour in the Ekman layer, or by surface fluxes proportional to the surface wind speed. Intensification is achieved both ways. In the former case, the inner part of the vortex intensifies while in the latter case, the circulation is concentrated in a ring-shaped area. An area of sinking motion in the center may lead to formation of an "eye".

1. Introduction

The idea that intensification of polar lows may be caused by CISK, has been set forth by Rasmussen (1979), Bratseth (1985) and others. The basic assumption is that water vapour convergence in the Ekman layer is converted to a corresponding amount of sensible heat. On the basis of quasi-geostrophic theory, the convergence of moisture is parameterized to be proportional to the relative geostrophic vorticity in the boundary layer.

Polar lows usually develop in a cold air mass located over a considerably warmer ocean surface. Assuming that the air mass is sufficiently stable aloft, a well-defined convective layer develops. Such a layer is characterized by being well-mixed with respect to equivalent potential temperature and mixing ratio, and is topped by an inversion, through which ambient air entrains the layer (Schubert et al., 1979). Under such conditions the cumulus convection will be confined to the convective layer, and the same should be true for a CISK model for growth of a disturbance (see, however, Økland, 1987).

A consequence of the arguments above is that the heating coming from the moisture convergence in the Ekman layer is only a part of the total heat flux from the ocean. These fluxes of sensible and latent heat in about the same amount are tied to the synoptic scale circulation, since their intensity increases with increasing wind speed. Because of the continuous convection, the sensible heat is distributed through a vertical air column in the same location as the corresponding flux. The same is not necessarily true for the latent heat, since it must be converted to sensible heat by condensation and part of the water vapour may be advected to another location before this happens. Furthermore, cloud drops may evaporate and thereby cool the air. In general, therefore, the synoptic scale heating by condensation under such conditions is quite complicated, and we shall not here make any effort to study this in detail. A more thorough discussion may be found in another paper of this volume (Økland, 1987). As a basis for the parameterization, we simply assume that one part of the overall heating of an air column is proportional to the geostrophic vorticity in the 1000 hPa surface, wherever the vorticity is positive, and that another part is proportional to the geostrophic wind speed at the same level. When numerical values are needed, we shall assume that the first part represents the latent heat release, while the second part represents the flux of sensible heat only.

Based on some general arguments and a simple

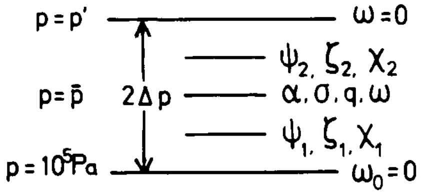

Fig. 1. Cross section showing the structure of the model.

two-layer model we shall show that the two heating terms have totally different effect on an existing barotropic vortex. In particular, the inclusion of heating proportional to the surface wind speed leads to downward motion in the central part of the low.

2. The effect of heating on an existing vortex

For the study in this paper we use a two-layer model with an intrinsic geostrophic balance between pressure and non-divergent wind (Lorenz, 1960). The equations are

$$\frac{\partial \zeta_1}{\partial t} = -J(\psi_1, \zeta_1) - \nabla \cdot [(1 + \zeta_1) \nabla \chi_1] \tag{1}$$

$$\frac{\partial \zeta_2}{\partial t} = -J(\psi_2, \zeta_2) - \nabla \cdot [(1 + \zeta_2) \nabla \chi_2] \tag{2}$$

$$\frac{\partial \psi'}{\partial t} = -J(\bar{\psi}, \psi') + \omega + Q, \tag{3}$$

where $\bar{\psi} = \frac{1}{2}(\psi_1 + \psi_2)$ and $\psi' = \frac{1}{2}(\psi_2 - \psi_1)$. The equations have been made non-dimensional, using f^{-1}, R_* and Δp as scales. Here

$$R_* = \Delta p f^{-1} (\sigma/2)^{1/2}$$

is the Rossby deformation radius, and $\sigma = -\alpha \partial \ln \theta / \partial p$, the stability parameter, is considered as a constant. Note that this conforms approximately with the conditions in the convective boundary layer (Økland, 1987), but disagrees with Lorenz' energy conserving model (Lorenz, 1960). The diabatic heating term, Q, will be defined presently. The rest of the symbols have the conventional interpretation, which partly may be inferred from Fig. 1. At the mid level an equation for ω (not included here) may be derived in the usual way. The boundary conditions are $\omega = 0$ at the top and bottom of the model, meaning that we do not consider the retarding effect of surface friction.

According to the discussion in Section 1, we consider the diabatic heating to consist of two parts:

$$Q = S v_0 + C \zeta_0, \tag{5}$$

where S is a positive constant and C is another constant, positive when $\zeta_0 > 0$ and zero when $\zeta_0 < 0$. Here v_0 and ζ_0 are the geostrophic wind and the geostrophic relative vorticity at $p_0 = 10^5$ Pa. The two terms will be referred to as the flux term and the CISK term, respectively.

For simplicity we consider a circular vortex which initially is barotropic through the convective boundary layer. Because of differential heating it gradually becomes baroclinic. We shall study the corresponding change in the circulation. Since the heating is tied to the 1000 hPa wind and vorticity, these quantities will dominate the changes. We shall throw light upon these processes by means of a numerical experiment. However, at first we discuss some initial configurations of wind and vorticity which will give insight in the general problem.

It will be asumed that the vortex initially has cyclonic circulation and that the vorticity

$$\zeta(r) = \frac{dv}{dr} + \frac{v}{r} \tag{6}$$

is everywhere finite, has a maximum at the center and decreases monotonously with increasing r, becoming negative for $r > a$. It is easily seen that the azimuthal velocity, $v(r)$, is zero at the center ($r = 0$), while $v'(0) = \frac{1}{2}\zeta(0) > 0$. Furthermore, $v(r)$ increases with increasing r and obtains a maximum at some r_m smaller than a. Any linear combination of $v(r)$ and $\zeta(r)$, like $A\zeta(r) + v(r)$, where A is a positive constant, will have a maximum somewhere between 0 and r_m, moving closer to the center when A increases.

From the omega equation it is shown that in general sinking motion ($\omega > 0$) exists where the Laplacian of Q is positive, and vice versa. Heating proportional to ζ therefore forces a value of ω depending on

$$\nabla^2 \zeta = \zeta''(r) + r^{-1} \zeta'(r), \tag{7}$$

which is seen to be negative for small r and equal to $2\zeta''(0)$ at the center. The Laplacian of v, however, has a large positive value for small r and actually becomes infinite at the center. We, therefore, conclude that any heating parameter-

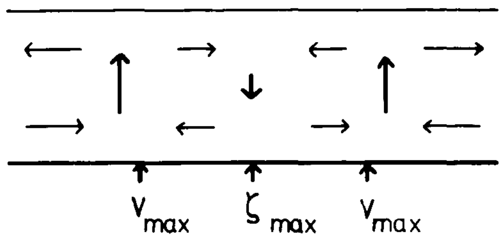

Fig. 2. Vertical cross section through the vortex, indicating the maximum of vorticity and wind speed, and the secondary circulation.

ized as a linear combination of terms proportional to ζ and v, leads to an area of sinking motion in the inner part of the vortex, this part being large when the term proportional to v is the most important one, and shrinking towards zero when the term vanishes.

It has already been established that v has a maximum somewhere in $r < a$. The Laplacian of v has a minimum at a slightly larger radius. This may, for instance, be seen from an expression for $\nabla^2 v$ similar to (7), and has an important consequence which will be described in the next paragraph.

The secondary circulation produced by the heating is shown schematically in Fig. 2. In general, in the lower half of the vortex there must be a "spin-down" domain in the inner part and a "spin-up" domain in the outer part. The associated change in the surface wind influences the heating. The spin-up area leads to an outward displacement of the ring with maximum heating. The circumstance that the Laplacian of the heating is at a somewhat larger radius, increases this effect. Some aspects of this development will be demonstrated in Section 3.

3. A numerical example

A grid-point version of the model was available, and was used for the experiments although a model based on circular symmetry might have been more appropriate. Initial values are derived from

$$\psi_1 = \psi_2 = D \exp(-r^2/a^2), \tag{8}$$

where r is the distance from the center of rotation and $a = 1.65\ 10^5$ m in dimensional space. Isolines of the corresponding height of the bell-shaped

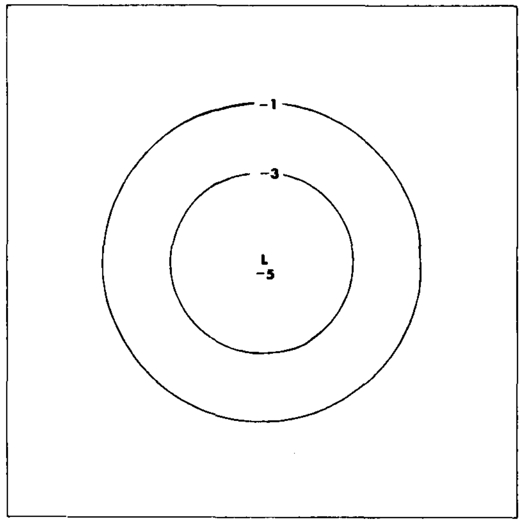

Fig. 3. Map of the initial value of the absolute topography, z_0, of the 1000 hPa surface. The unit is decameter.

pressure surface is shown in Fig. 3. The model top is at 600 hPa. Other characteristics of the integration may be found in the Appendix.

Based on (8) the radial variation of the two terms in (5) may be computed. The result is shown in Fig. 4 as a thin continuous line and a broken line. For easy comparison the two curves have been scaled to the same maximum value. Also shown as a heavy continuous line is the scaled value of Q used in the integration. Note that these curves represent initial values which

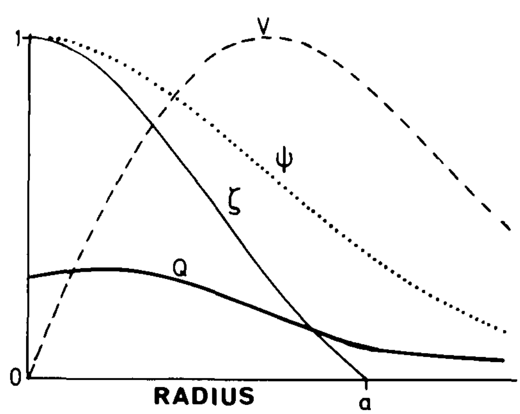

Fig. 4. Radial variation of ζ_0 (thin line), v_0 (broken line), Q (heavy line) and ψ (dotted line).

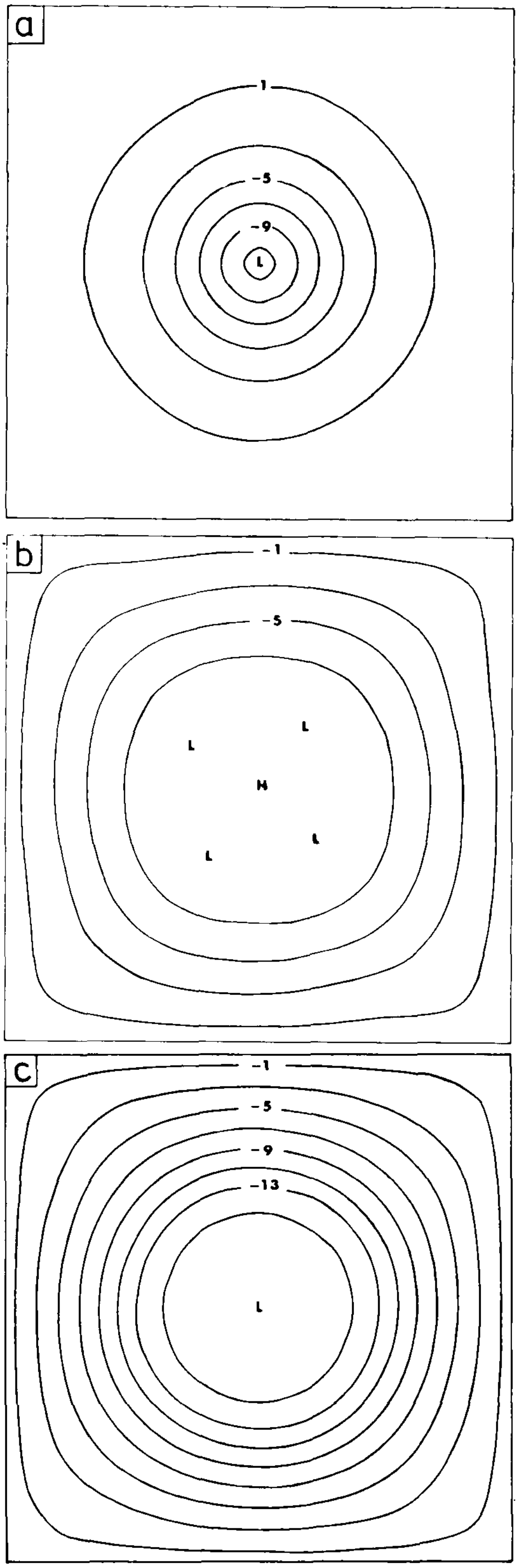

will be changed during the integration. The dotted line pictures the initial profile of ψ for comparison. Some of the deductions in the previous section are clearly reflected in the figure, for instance the displacement of the maximum heating rate away from the center when the flux term is included.

Figs. 5a, b, c, show the 1000 hPa height after 24 h simulated time for different values of the constants S and C in (5). This particular pressure surface has been derived from prognostic values of ψ_1 and ψ_2 by extrapolation. The result should be compared to the initial values on Fig. 3. As expected, the CISK term alone leads to a strong intensification of the inner part of the vortex (Fig. 5a). In striking contrast to this case, Fig. 5b shows the result when only the flux term is included. The circulation has virtually vanished in the interior of the vortex and is concentrated in a peripheral ring-shaped area. (The 4 lows surrounding the central high are caused by truncation errors associated with the representation of a circular vortex in a square grid.) Finally, Fig. 5c shows the corresponding result when both terms are present. Obviously, the general structure is somewhere between the two previous cases, but the circulation is much stronger, as a consequence of the fact that the total heating rate is larger than in the two previous cases. This simulation is in good agreement with those obtained by Aakjær and Rasmussen (1985).

4. Conclusions

In this paper, we have tried to show that heating depending on the surface heat fluxes, and accordingly increasing with the surface wind speed, may have considerable influence on a vortex. It may be responsible for the "eye" often noted in case studies of polar lows, since it creates subsidence in an area around the low center, this area being small when the flux is relatively small. The tendency to displace the active part of the

Fig. 5. Maps of the absolute topography, z_0, after 24 h simulated time with (a) heating proportional to ζ_0, (b) heating proportional to v_0, and (c) the combination. The unit is decameter.

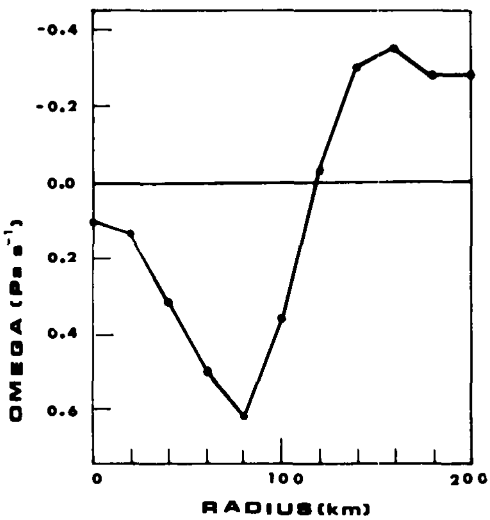

Fig. 6. Radial variation of ω after 24 h.

low from the center to more peripheral areas is clearly demonstrated by the profile of ω at 24 h simulated time pictured in Fig. 6. Since the circular symmetry is not strictly conserved during the integration, the grid-point values have been interpolated to circles at different radii. Here we see an area with downward motion in the inner part of the low, while the upward motion is displaced outward. In contrast, heating proportional to the relative vorticity (CISK) tends to form an intense vortex in the central part of the low.

5. Acknowledgement

This study has been supported financially by the Norwegian Meteorological Institute as a part of the Polar Lows Project.

6. Appendix

Numerical values used in the numerical experiment

$\Delta p = 200$ hPa
$\sigma = -\alpha \partial \ln \theta / \partial p = 0.67 \times 10^{-6}$ m^2 s^{-2} Pa^{-2}
$f = 1.3 \times 10^{-4}$ s^{-1}
R_* (Rossby deformation radius)
$\Delta p f^{-1} (\sigma/2)^{1/2} = 89$ km
$\bar{p}$ (reference pressure) = 800 hPa
$\rho_0 = 1.3$ kg m^{-3}
C_H (transfer coefficient for heat) = 0.002
ΔT (air-sea temperature difference) = 10 K
$\kappa = 0.286$

The heating term in the scaled equation (3) is expressed as

$$Q = \frac{\kappa}{2} \frac{\Delta p}{\bar{p}} R_*^{-2} f^{-3} q.$$

Here q is heat transfer to the air per kg per s, related to the total heat transfer to a column by the relation

$$H = \frac{2\Delta p}{g} q.$$

In the flux term H is expressed as

$$H = c_p \rho_0 C_H (\Delta T) R_* f |\nabla \psi_0|,$$

where $|\nabla \psi_0|$ is the scaled surface geostrophic wind.

The convergence of mass in the Ekman layer is related to the dimensional geostrophic vorticity through the relation

$$\omega_E = -f(\delta p)\zeta,$$

where ω_E refers to the "top of the Ekman layer" and $(\delta p) = 1300$ Pa in the calculations. Then

$$H = g^{-1} L_c m f(\delta p)\zeta,$$

where L_c is the latent heat of condensation, $m = 0.003$, a characteristic value of water vapour mixing ratio in the Ekman layer, and ζ is non-dimensional.

REFERENCES

Aakjær, P. and Rasmussen, E. 1985. Modelling of polar lows in a barotropic environment using the Danish operational limited area model. Report No. 6, Weather Service, Danish Meteorological Institute, Copenhagen, 50 p.

Bratseth, A. M. 1985. A note on CISK in polar air masses. *Tellus 37A*, 403–406.

Lorenz, E. N. 1960. Energy and numerical weather prediction. *Tellus 12*, 364–373.

Økland, H. 1987. Heating by organized convection as a source of polar low intensification. *Tellus 39A*, 398–408.

Rasmussen, E. 1979. The polar low as an extratropical CISK-disturbance. *Q. J. R. Meteorol. Soc. 105*, 531–549.

Schubert, W. H., Wakefield, J. S., Steiner, E. J. and Cox, S. K. 1979. Marine stratocumulus convection. Part II: Horizontally inhomogeneous solutions. *J. Atmos. Sci. 36*, 1308–1324.